JOURNAL OF GEOPHYSICAL RESEARCH, VOL. 93, NO. D5, PAGES 5319–5332, MAY 20, 1988

Effects of Dirty Snow in Nuclear Winter Simulations

A. M. VOGELMANN,[1] A. ROBOCK, AND R. G. ELLINGSON

Department of Meteorology, University of Maryland, College Park

A large-scale nuclear war would inject smoke into the atmosphere from burning forests, cities, and industries in targeted areas. This smoke could fall out onto snow and ice and would lower cryospheric albedos by as much as 50%. A global energy balance climate model is used to investigate the maximum effect these "dirty snow" albedos have on the surface temperature in nuclear winter simulations which span several years. These effects are investigated for different nuclear winter scenarios, snow precipitation rates, latitudinal distributions of smoke, and seasonal timings. We find that dirty snow, in general, would have a small temperature effect at mid- and low latitudes but could have a large temperature effect at polar latitudes, particularly if the soot is able to reappear significantly in later summers. Factors which limit the climatic importance of the dirty snow are (1) the dirty snow albedo is lowest when the atmosphere still contains a large amount of light-absorbing smoke; (2) even with dirty snow, sea ice areas can still increase, which helps maintain colder temperatures through the sea ice thermal inertia feedback; (3) the snow and ice areas affected by the dirty snow albedos are largest when there is little seasonal solar insolation; and (4) the area affected by the dirty snow is relatively small under all circumstances.

1. INTRODUCTION

Nuclear winter theory suggests that large amounts of smoke and dust could be injected into the atmosphere as a result of a major nuclear exchange [*Crutzen and Birks*, 1982; *Turco et al.*, 1983]. These aerosols would absorb solar radiation in the upper atmosphere and could cause large drops in the surface temperature as well as other climatic perturbations (see *National Research Council (NRC)* [1985] and *Pittock et al.* [1986] for a review).

Several studies have shown that snow and ice areas could play an important role in the climate's response to hypothesized nuclear winter forcings. *Robock* [1984*b*] used an energy balance climate model (EBCM) to show that the cooling caused by this forcing could be enhanced by the well-known positive feedback of snow and ice areas on surface temperature. The initial nuclear winter cooling causes the cryospheric areas to increase. These anomalous areas raise the planetary albedo, and the formation of more sea ice reduces the ocean's thermal inertia. This causes lower temperatures and these lower temperatures persist after the nuclear winter forcing has dissipated, because of the thermal inertia of the ocean and the time lag required to melt the sea ice and snow. These feedbacks were also found to operate in nuclear winter experiments conducted with a general circulation model (GCM) [*Covey*, 1987].

The high albedo of pure snow can be reduced by a few percent when mixed with only 1 part per million (ppm) of carbon soot by weight [*Warren*, 1982, 1984; *Warren and Wiscombe*, 1980; *Chylek et al.*, 1983]. In the case of nuclear winter theory, millions of tons of smoke, composed largely of carbon soot, could be injected into the atmosphere. When this smoke is removed from the atmosphere, large quantities of soot could be deposited on snow and ice fields, significantly lowering their albedos [*Crutzen and Birks*, 1982]. *Warren and Wiscombe* [1985] calculated how the snow albedos could change when mixed with different weight fractions of nuclear winter smoke. They showed that for the scenarios used, a clean snow albedo of 0.84 could drop to a "dirty snow" value of 0.50. Such an albedo change could have a large climatic effect, particularly in the high latitudes.

Ledley and Thompson [1986] applied the albedo results of Warren and Wiscombe to a one-dimensional thermodynamic sea ice model to examine the effect "smokefall" could have on the seasonal variation of sea ice in a clean atmosphere. The model, among other things, explicitly computed the energy fluxes at the ice interface, the change in ice thickness, and the albedo change as snow accumulated on the soot layer. The model also allowed the soot to reappear if the blanketing layer of snow melted. They found that the period of ice-free oceans at high latitudes could increase by 0.3–3.5 months, depending on the timing of the smokefall and the latitude. The greatest effects were found in April and January when the ice areas are largest.

The previous studies have not examined the climatic effects of the dirty snow while considering the concurrent effects of the atmospheric smoke cloud. The presence of the smoke cloud could be important to the dirty snow effect by reducing the amount of energy available for absorption at the surface [*Warren and Wiscombe*, 1985]. Also, in previous models the smoke was deposited at a constant rate over different periods of time, thus not including the projected lifetimes of the smoke particles nor the evolution of the dirty snow albedos.

This work considers the importance of the dirty snow albedos with a global climate model which includes the concurrent effects of the smoke cloud. A dirty snow parameterization is used which considers the long-term deposition of the smoke, as dictated by its atmospheric residence times. To investigate both short- and long-term effects, different

[1]Now at Atmospheric and Environmental Research, Incorporated, Cambridge, Massachusetts.

Paper number 8D0074.
0148-0227/88/008D-0074$05.00

nuclear winter scenarios, latitudinal distributions, snow precipitation rates, and seasonal timings are used.

In section 2 of this paper, the climate model and the modifications made to include the nuclear winter smoke cloud are described. The nuclear winter scenarios used are then discussed in section 3, and section 4 explains how the dirty snow albedos were calculated and incorporated in the climate model. The results of the climate model experiments are given, in section 5, which illustrate the climatic effects of the dirty snow. Section 6 contains the summary and discussion.

2. Climate Model

The global energy balance climate model used here is based on *Sellers* [1973, 1974] with changes made as indicated by *Robock* [1983]. The seasonal cycle is resolved by 24 time steps, each approximately 15 days long. The globe is composed of 10° latitude bands, each with a separate, zonally averaged land and sea component. In the radiation model there are three layers in the vertical, one for the surface and two for the atmosphere. A detailed surface albedo parameterization is used which includes snow, ice, and meltwater area feedbacks. The extent of the snow and ice areas are calculated with separate regression equations, based on a fit of the surface temperature to the observed cover [*Robock*, 1980, 1983]. These regression equations treat only the fractional area covered by the snow or ice and do not explicitly calculate snow depth or sea ice thickness.

The model uses assumptions and parameterizations which, although enabling it to reproduce the current climate, may impede the model's ability to accurately simulate climates very different than the present. For example, the model has a poor vertical resolution, which will not allow it to resolve intense inversions, the cloud cover is fixed at the bimonthly climatology, and the sea is represented with a simple mixed layer ocean model which has a constant depth throughout the year. Since this is not a GCM, atmospheric dynamics are parameterized. Because of these and other restrictions, these model simulations are best regarded as sensitivity experiments which are indications of the climate system's potential response to the forcing.

These sensitivity experiments, although not entirely realistic climate simulations, can provide useful information. The model's coarse spatial resolution allows it to be run very quickly and thus makes it possible to perform long-term experiments. Because of this computational efficiency, many different experiments can be made to further investigate the reasons for the resulting patterns The model's simplicity also allows one to analyze the effects of different forcings more easily than is possible with more complicated models like general circulation models.

To make nuclear winter simulations, a third atmospheric layer containing only smoke and dust was added to the top of the climate model. The assumption that these aerosols are very high in the atmosphere is reasonable for long-term climate experiments since only the aerosols in the upper troposphere and the stratosphere would have long residence times [*Ghan et al.*, 1985; *Malone et al.*, 1986; *Thompson et al.*, 1986]. The smoke layer does not contain atmospheric gases, so it vanishes when the optical depth of the smoke and dust is zero.

A gray optical depth in the visible is assigned to the smoke layer for each 10° latitude band at every time step. The reflectivity and transmissivity of the smoke cloud are calculated from the solutions to the two-stream approximation [*Sagan and Pollack*, 1967]. The longwave (wavelengths > 4 μm) optical depth is assumed to be one tenth of the visible extinction optical depth. The emissivity is 1 minus the transmission, where the infrared optical depth is multiplied by the diffusivity factor of 5/3 [*Lacis and Hansen*, 1974]. The smoke cloud is treated as an isothermal layer, so the downward longwave flux may be overestimated (assuming a temperature inversion in the smoke layer).

The shortwave radiation absorbed by the aerosol cloud is calculated (including the effects of multiple reflections) and the sensible, latent, and advective heatings are assumed to be zero, since this layer is high in the atmosphere, where conditions are relatively stable. The smoke cloud's absorption and emission of longwave radiation are coupled to the other atmospheric layers of the model, assuming radiative equilibrium. The downward longwave flux from the smoke cloud, not included in the previous model version [*Robock*, 1984*b*], is thus considered. The temperature response of the smoke cloud is calculated separately for clear and cloudy (water) conditions over both the land and sea areas in each latitude band.

3. Nuclear Winter Scenarios

Established nuclear winter scenarios are used to force the climate model, since it cannot perform particle scavenging calculations. This study uses the baseline scenarios of *Turco et al.* [1983], the *NRC* [1985], and extrapolations of the *Malone et al.* [1986] GCM results.

In the Turco et al. scenario and the National Research Council scenario (hereafter referred to as the TTAPS and NRC scenarios, respectively), the initial, instantaneous vertical distribution of the smoke, its washout rate, and its horizontal extent were prescribed using best estimates. In the TTAPS scenario, 225 Tg of smoke were injected into the atmosphere, and in the NRC scenario, 180 Tg of smoke were used. The Malone et al. GCM experiments used 170 Tg of NRC smoke and the initial NRC vertical distribution but, in contrast to the prescribed NRC and TTAPS scenarios, the GCM calculated the interactive movement and scavenging of the smoke by model-calculated winds and precipitation (also see *Ghan et al.* [1985] and *Thompson et al.* [1986]). Thus these GCM simulations give estimates of the smoke's horizontal distribution and atmospheric lifetime which are probably more realistic than the prescribed scenarios. The results of Malone et al. show that 65–85% of the aerosols initially injected in the atmosphere could be quickly washed out. After the initial washout, the remaining aerosols could have a prolonged atmospheric lifetime due to their absorption of solar radiation which heats the surrounding air and transports the aerosols to higher altitudes (smoke lofting). These model results also showed that the smoke (initially injected only over the northern hemisphere) could spread into the southern hemisphere and it was estimated that after many months, a thin layer of smoke could uniformly cover the globe.

The effects of the TTAPS and NRC nuclear winter forcings were tested when instantly distributed uniformly over the northern hemisphere. To construct the Malone et al. scenarios, the optical depths from the published GCM runs (at day 20 for January and day 40 for July) were extrapolated in time using the e-folding times given in their paper

(1.5 months for January and 6 months for July). In these extrapolations the smoke was not allowed to spread horizontally because of the difficulty in projecting, with any meaningful degree of certainty, the complicated dynamical interactions of the winds and smoke. This overestimates the optical depths in the northern hemisphere and underestimates those in the southern hemisphere The initial optical depths for both summer and winter are lower for the Malone et al. scenarios for both winter and summer than for NRC or TTAPS. By day 100 of the simulations, the Malone et al optical depth for summer becomes larger than for the NRC case. For winter, the Malone et al. optical depths are always smaller than all the others

Because the smoke distribution and washout are prescribed in the NRC and TTAPS scenarios, it is possible to calculate the long-term smoke deposition needed for dirty snow calculations. Dirty snow calculations are not possible with the Malone et al. scenarios because of a lack of information concerning the smokefall. These extrapolations, however, are still useful to obtain a more accurate estimate of the possible nuclear winter coolings. This provides a standard for comparison of the TTAPS and NRC scenarios used for the dirty snow experiments.

4. DIRTY SNOW

Dirty snow albedos depend on the weight fraction of soot in snow the greater the weight fraction, the lower the snow albedo. To obtain this weight fraction, the amount of soot and snow which have fallen in every 15-day time step are required In this section, the calculation of "sootfall," snowfall, the resulting dirty snow albedos, and the incorporation of these dirty snow albedos into the climate model are discussed (The term "dirty snow" is used as a generic term which includes dirty ice and dirty meltwater albedos)

4 1. *Sootfall and Horizontal Distribution*

The smokefall in the NRC and TTAPS scenarios is calculated for each 15-day time step from the prescribed vertical injection profiles and washout rates. The sootfall is then calculated for each time step, knowing that the NRC smoke is composed of 20% NRC soot (by mass) while the TTAPS smoke would have to be 50% NRC soot to be consistent with published optical data [*NRC*, 1985, Table 5.7]. The soot is deposited at the surface only at the latitudes where the smoke cloud is present. These calculations assume that the soot is removed only by precipitation scavenging. Laboratory experiments indicate that soot would not be removed by chemical oxidation [*Stephens et al.*, 1988].

To see how credible the calculated smokefall is for the prescribed NRC and TTAPS scenarios, they were compared to the more realistic, one month interactive GCM smoke-scavenging calculations of Ghan et al. (S. Ghan, personal communication, 1985). For this comparison the smokefall in the NRC and TTAPS scenarios was uniformly distributed over the northern hemisphere The hemispherically distributed prescribed scenarios (NRC, TTAPS), compared to the GCM runs in January or July, overestimate the amount of smokefall at the snow-covered high latitudes. This is because the fast washout in the GCM runs quickly cleanses a majority of the smoke from the atmosphere and deposits it at its source region in the mid-latitudes. (After this initial washout, smoke lofting markedly slows the deposition rate of the the remaining smoke in the GCM simulations) After 15 days, the smokefall in the prescribed cases exceeds that in the GCM runs everywhere (even in the mid-latitudes), since more smoke remained in the atmosphere without the fast initial washout. The prescribed hemispheric cases then overestimate the amount of smokefall in the higher latitudes and its longevity everywhere.

4.2. *Snowfall*

The snowfall rate is not calculated by the climate model, so it is parameterized. It is difficult to estimate what the long-term precipitation changes could be after such a perturbation The present-day snowfall rates over the Arctic Ocean and Greenland are 10 kg m^{-2} $month^{-1}$, and 30 kg m^{-2} $month^{-1}$, respectively [*Warren and Wiscombe*, 1985]. (Ten kilograms per square meter per month of precipitation is equal to 1 cm of liquid water per month or, if it were all snow, about 10 cm of snowfall per month.) These rates are smaller than those in most regions of the world. *Ghan et al.* [1985] showed that the precipitation in a nuclear winter could be dramatically reduced over land areas, while being increased over the ocean areas

From these considerations, a baseline precipitation rate of 10 kg m^{-2} $month^{-1}$ and an excursion value of 30 kg m^{-2} $month^{-1}$ are used. The baseline value chosen is on the lower end of the perturbed land precipitation rates shown by Ghan et al and thus yields a maximum dirty snow effect. In the climate model it is assumed that all precipitation over the snow and ice fields is snow and that this snowfall is uniformly mixed with the amount of soot deposited during that time step.

4 3. *Dirty Snow Albedos*

Warren and Wiscombe [1985] calculated the spectrally averaged albedos of snow when uniformly mixed with different amounts of NRC soot. Their calculations assume that the soot particles reside only outside the ice grains (externally mixed) which, they stated, would underestimate the albedo change of the more likely situation that the soot resides both outside and inside the ice grains (If the soot resides only inside the ice grains, it takes only half the soot mass of a purely external mixture to yield the same albedo) The albedo effect of dust being mixed with the snow is not considered here, since soot is 50 times more effective at reducing snow albedos [*Warren*, 1984]. The dust, however, could be important in masking the lower albedo of soot

Dirty snow, ice, and meltwater albedos, as a function of the soot concentration in snow, were interpolated from the results of Warren and Wiscombe, so that the clean values matched those used in our climate model (Figure 1) The meltwater curve parameterizes the albedo effects as the snow and ice age and melt, based on observations. This includes, in a gross way, the formation of water puddles, the accumulation of impurities at the surface, and, in the case of ice, the appearance of leads (open water). This parameterization does not account for the possibility that the soot is washed off the snow or ice surfaces during melting. Nor does it account for observations which show that fine dust and soot particles tend to accumulate at the surface during the melting process, altering the albedo [*Warren*, 1984]

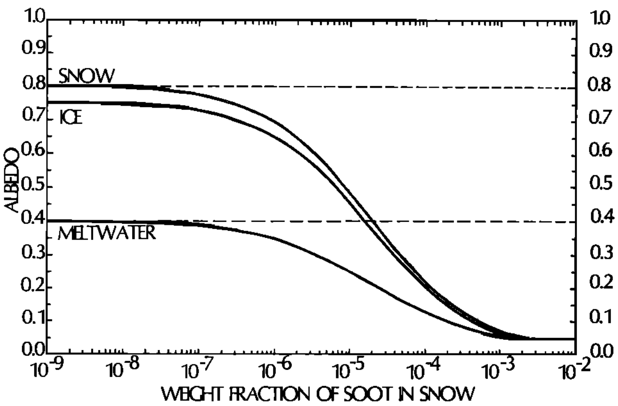

Fig. 1. Dirty snow, ice, and meltwater albedos as a function of the soot content. (The ice areas are assumed to be partially covered with snow.) Albedos are spectrally averaged using the solar spectrum at sea level for a subarctic summer standard atmosphere. Curves are interpolated from the results of *Warren and Wiscombe* [1985]. Albedos are obtained by interpolating lines which start at "clean snow" albedos (0.80, 0.75, 0.40 for the snow, ice, and meltwater albedos, respectively) and keep the same fractional distance between the new snow curve (of Warren and Wiscombe's graph) and the pure soot albedo of 0.05.

Using this information, the dirty snow albedos were calculated as a function of time for the TTAPS and NRC scenarios assuming different latitudinal distributions and snowfall rates (Figures 2 and 3) The TTAPS dirty snow albedos are lower and longer lasting than the NRC albedos because there is more smoke injected into the atmosphere, the smoke has a longer atmospheric residence time, and it has a greater absorption coefficient

The dirty snow albedos used by *Ledley and Thompson* [1986] are lower than those found here. This is because the smoke in this study was deposited over a longer period of time in a manner consistent with its atmospheric lifetime. (The smoke was deposited in only 1 month for their sea ice model runs.) Also, our work and Ledley and Thompson's both interpolate albedo curves from the results of Warren and Wiscombe. Our interpolations assume a slightly smaller change in albedo with soot content than Ledley and Thompson's.

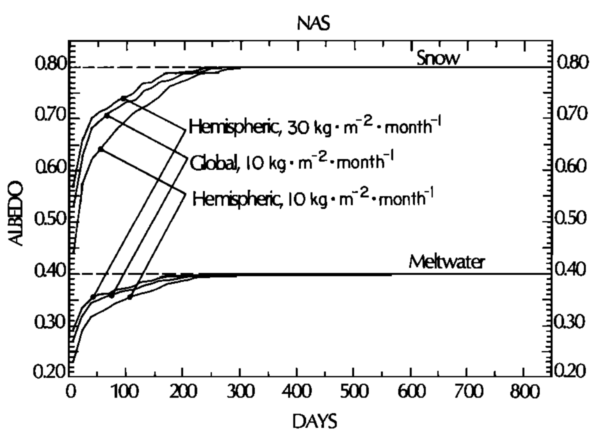

Fig. 2. Dirty snow and meltwater albedos as a function of time for the NRC scenario. The snowfall rate and the smoke's horizontal distribution are indicated for each pair of curves. The snowfall rate is constant over time for each curve.

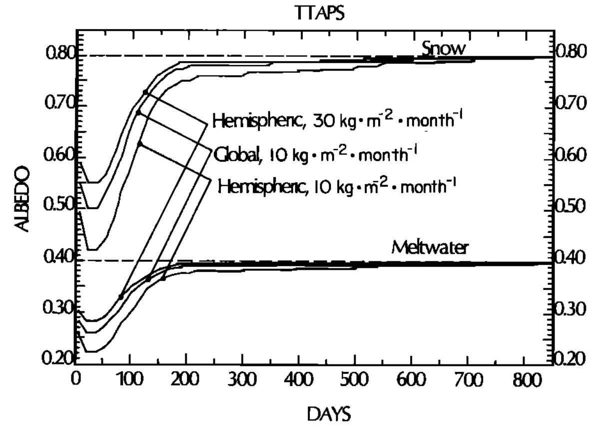

Fig. 3. As in Figure 2, but for the TTAPS scenario. The large dip in these albedo curves is caused by a layer of higher smoke concentration which has settled to the ground. (A similar layer does not result from the NRC vertical injection profile.)

4.4. *Climate Model Parameterization*

In the climate model it is assumed that for each time step, the new layer of dirty snow completely blankets the old layer, since there is little difference in their albedos The soot not falling on snow or ice areas does not cause an albedo change. As the snow melts, snow and ice albedos change linearly with temperature from their value at $T < -10°C$ to the corresponding meltwater value at $T > 0°C$ [*Robock*, 1980]. Because the meltwater albedo is already low, albedo change when the soot is introduced will be smaller than in the case with no meltwater. The climate model does not calculate the depth of the snow, so it is not possible to explicitly calculate the reappearance of soot covered by clean snow. This process is approximated, however, in sensitivity experiments discussed later.

5. MODEL RESULTS

In this section the temperature drops caused by the different nuclear winter scenarios are compared. The first model runs are conducted only with clean snow to examine the qualitative differences in the forcings caused by the different smoke distributions. The effects of dirty snow on this cooling are then discussed. See Table 1 for a summary of the sections and the results shown.

5.1. *Nuclear Winter Forcings*

The NRC, TTAPS, and *Malone et al.* [1986] scenarios are used to force the climate model to evaluate the plausible magnitudes of the nuclear winter cooling, as predicted by this model. These model runs were all done using clean snow. Of particular interest is how the coolings from the prescribed scenarios (used later for the dirty snow experiments) compare to the more realistic Malone et al scenarios. The temperature drops (or cooling) caused by the nuclear winter forcing are displayed by subtracting the unperturbed model climatology from the surface air temperature of the forced model run. The results shown here are zonally averaged over the land and sea areas, although the climate model calculates land and sea surface air temperatures separately. (The cooling minima for the separate land and

TABLE 1. Model Results Shown

Figure Number	Forcing[a]	Horizontal Distribution	Started	Field Shown[b]
		Nuclear Winter Forcings		
4*a*	NAS	0–90°N	July	cooling[c]
4*b*	TTAPS	0–90°N	July	cooling
4*c*	Malone	GCM[d]	July	cooling
5	TTAPS	0–90°N	January	cooling
		Scenario Dependence		
6*a*	TTAPS	0–90°N	January	albedo difference[e]
6*b*				cooling reduction[f]
7*a*	NAS	0–90°N	January	albedo difference
7*b*				cooling reduction
		Seasonal Dependence		
8*a*	TTAPS	0–90°N	July	albedo difference
8*b*				cooling reduction
9*a*	TTAPS	0–90°N	March	albedo difference
9*b*				cooling reduction
9*c*				cooling reduction of land
9*d*				cooling with dirty snow
		Smoke Cloud Absorption		
10	TTAPS	0–90°N	March	temperature difference[g]
		Soot Reappearance		
11*a*	NAS	0-90°N	March	albedo difference
11*b*				cooling reduction
11*c*				cooling with dirty snow[h]
11*d*				anomalous ice areas[i]
11*e*				ice area reduction[j]

[a] See text for explanation of forcing.
[b] All fields except Figure 9*c* are zonally averaged over both the land and sea areas.
[c] Temperature difference between the nuclear winter run (with clean snow) and model climatology.
[d] Horizontal distribution fixed at the final GCM distribution after 40 days.
[e] Albedo difference between the clean and dirty snow nuclear winter runs.
[f] Temperature difference between the clean and dirty snow nuclear winter runs.
[g] Temperature difference between the clean and dirty snow clean-atmosphere runs.
[h] Temperature difference between the nuclear winter run (with dirty snow) and model climatology.
[i] Ice area difference between the nuclear winter run (with clean snow) and model climatology.
[j] Ice area difference between the clean and dirty snow nuclear winter model runs.

sea areas in the first year are approximately 150% and 50% of the zonally averaged cooling minimum, respectively After the first year, the pattern of the zonal cooling closely represents that for either the sea or land areas)

The scenarios are first started in July, with the NRC and TTAPS forcings distributed uniformly over the northern hemisphere, and with the Malone et al forcing retaining its horizontal extent at the end of the 40-day GCM experiment From these results, the NRC cooling (Figure 4*a*) is less and shorter-lasting than the TTAPS cooling (Figure 4*b*) This is because more smoke is injected into the atmosphere in the TTAPS scenario, it stays in the atmosphere longer, and it absorbs solar radiation better than the smoke in the NRC scenario. Note that cooling is possible in the southern hemisphere (where there is no direct forcing) as a result of the heat transport across the equator. The initial cooling of the Malone et al. run (Figure 4*c*) is smaller than in either of the prescribed scenarios (due to the fast washout), but the long-term cooling is intermediate to that in the TTAPS and NRC scenarios (because of the long smoke residence time caused by the summertime smoke lofting).

When the hemispherically distributed NRC and TTAPS scenarios are started in January, there is much less cooling, because it is already cold in the northern hemisphere and there is little solar radiation for the smoke cloud to absorb (Figure 5 (TTAPS)). Note that warming initially occurs at the high latitudes since the smoke cloud does not reduce the solar flux reaching the ground in that region (none), but does trap the terrestrial radiation which normally escapes to space The NRC run (not shown) caused about half the cooling of the TTAPS run The January Malone et al run (not shown) causes virtually no cooling since the lack of solar radiation reduces the smoke lofting and allows the smoke to be quickly washed out of the atmosphere

In summary, the prescribed scenarios seem to provide a reasonable range for the nuclear winter forcing as compared to the GCM extrapolations. Presumably, these same scenarios would then also provide a reasonable range for the dirty snow modifications.

5.2. *Comparison With Other Simulations*

The amount of cooling found in the previously described model runs is systematically less than that found by other climate models for comparable nuclear winter scenarios [e.g. *NRC*, 1985; *Pittock et al.*, 1986]. There are several reasons for this difference One is that the climate model used here has a very low vertical resolution, preventing the simulation of strong surface temperature inversions with their resulting cold surface temperatures Another significant factor is that the model uses 15-day time steps, thus forcing the model with 15-day average optical depths and calculating 15-day

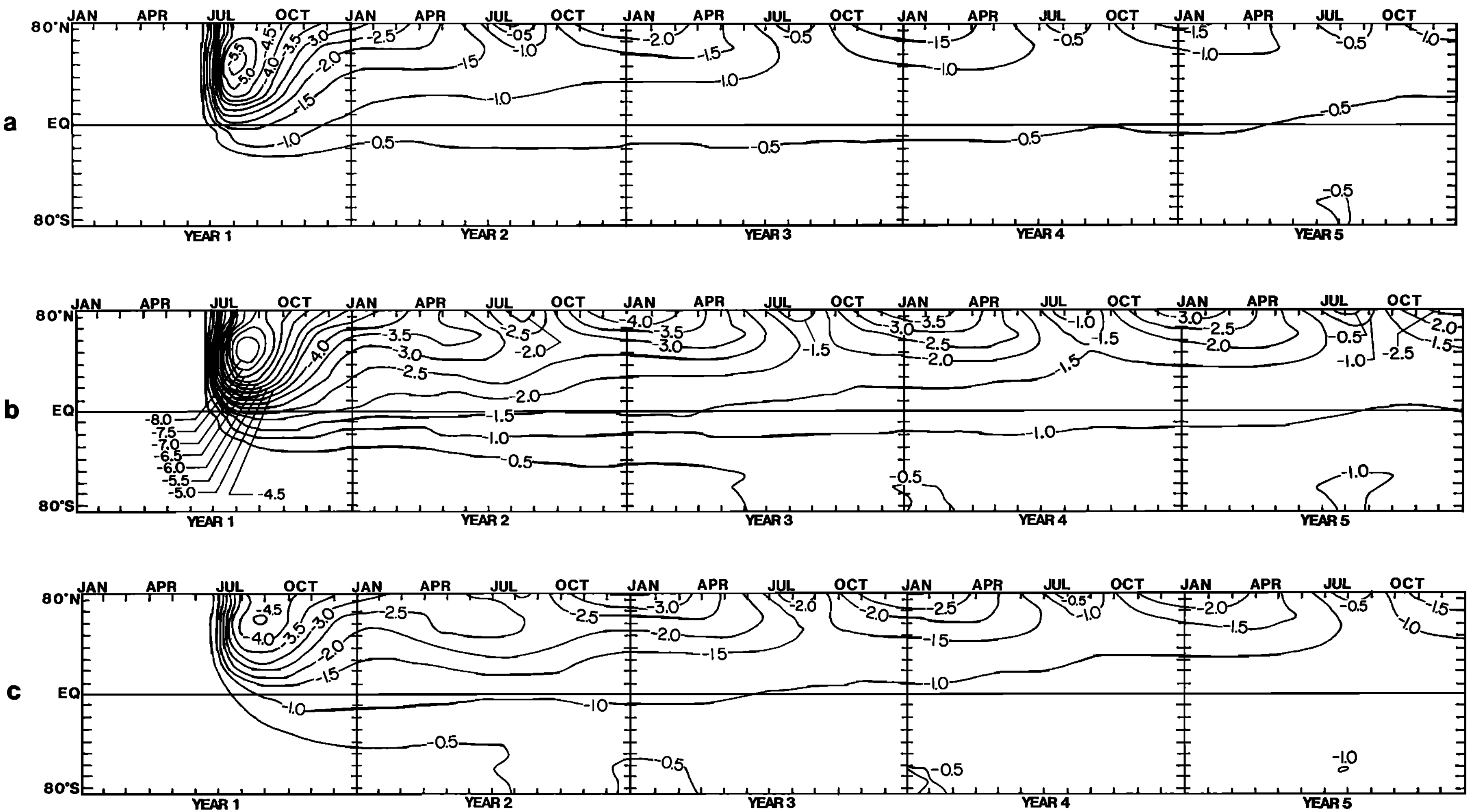

Fig. 4. Cooling for the nuclear winter scenarios started in July. Zonally averaged temperature differences (nuclear winter experiment minus unperturbed climate) are given as a function of latitude and time. Shown are (*a*) the hemispherically distributed NRC scenario, (*b*) the hemispherically distributed TTAPS scenario, and (*c*) the July *Malone et al.* [1985] scenario. Contours every 0.5°C, starting at -0.5°C. The effects which seem to preceed the start of the forcing are due to the finite width of the draftsman's pen and interpolations in the graphics routines.

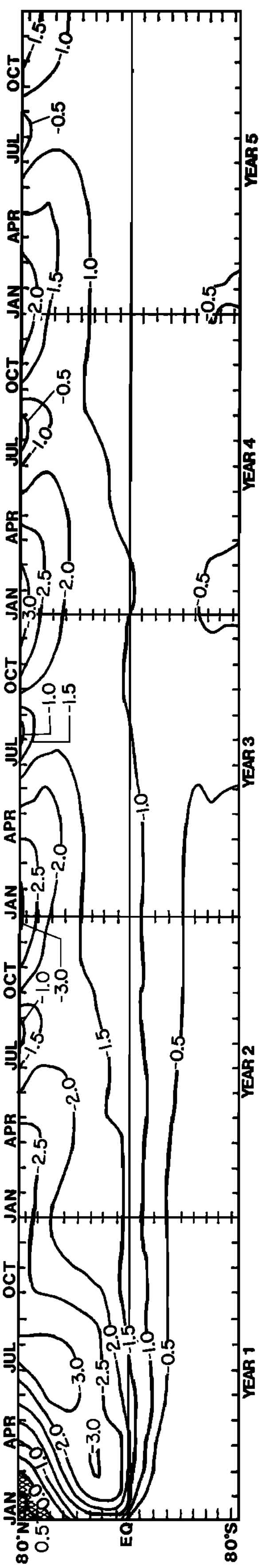

Fig. 5. As in Figure 4, but for the hemispherically distributed TTAPS scenario started in January. Region where warming occurs is hatched.

average climate response. This will smooth out the high optical depths and large surface temperature drops found in calculations which have several time steps per day. In addition, the downward infrared flux from the isothermal smoke layer used in these calculations is overestimated, as compared to a smoke layer with a temperature that increases with height. Also, soil heat capacity is included in our simulations, which would reduce the surface temperature response, an effect not included in the published GCM calculations. All of these factors reduce the short-term cooling of the model and would consequently reduce the longer-term cooling and the cryospheric feedbacks discussed in section 5.3. Finally, we display zonally averaged results, which include the lower temperature response over the oceans. Comparisons with other surface temperatures zonally averaged over land areas should multiply the coolings shown here by about 1.5, as discussed earlier. When comparing our coolings to maximum midcontinent coolings shown by others, our coolings should be increased by even more (2 – 4).

5.3. *Sea Ice Feedbacks*

A feature to note in the previous results is that after the direct nuclear winter forcing has ended (0.7 years for the NRC, 2.7 years for the TTAPS, and 2.0 years for the July Malone et al. case), cooling persists in all the experiments shown. This prolonged cooling is caused primarily by the ocean's sea ice thermal inertia feedback. The increased sea ice areas make the ocean more continental which allows it to cool more quickly, causing lower temperatures which, in turn, support the existence of anomalous cryospheric areas in a positive feedback loop This feedback has also been observed with this model when forced with volcanic dust veils [*Robock* 1981, 1984*a*] in previous nuclear winter experiments, which did not include the downward infrared flux from the smoke cloud [*Robock*, 1984*b*], and in data analysis of surface temperature response to volcanic forcing [*Robock*, 1985]. The response pattern, with the largest response at high latitudes in winter, is also found in equilibrium calculations with the same energy balance climate model for experiments changing the solar constant by 1% [*Robock*, 1983] and in GCMs for quadrupling CO_2 [e.g., *Manabe and Stouffer*, 1980]. It is caused by an amplified or reduced seasonal cycle in high latitudes as the extent of the ice cover of the ocean makes it more or less continental. *Covey* [1987] also finds these feedbacks in extended GCM nuclear winter experiments.

5 4. *Scenario Dependence*

The climate model was forced with the same scenarios as above but using dirty snow albedos Output fields from the nuclear winter runs with and without dirty snow were subtracted to display its net effect. The baseline precipitation rate of 10 kg m^{-2} $month^{-1}$ is used for the dirty snow calculations. The objective of these first experiments is to determine how the dirty snow's "cooling reduction" differs between the TTAPS and NRC scenarios.

The TTAPS scenario is started in January, with the forcing spread uniformly over the northern hemisphere. Figure 6*a* shows that the dirty snow can lower the surface albedo by as much as 0.3 in the high latitudes This "albedo difference" is virtually all due to the dirty snow and sea ice,

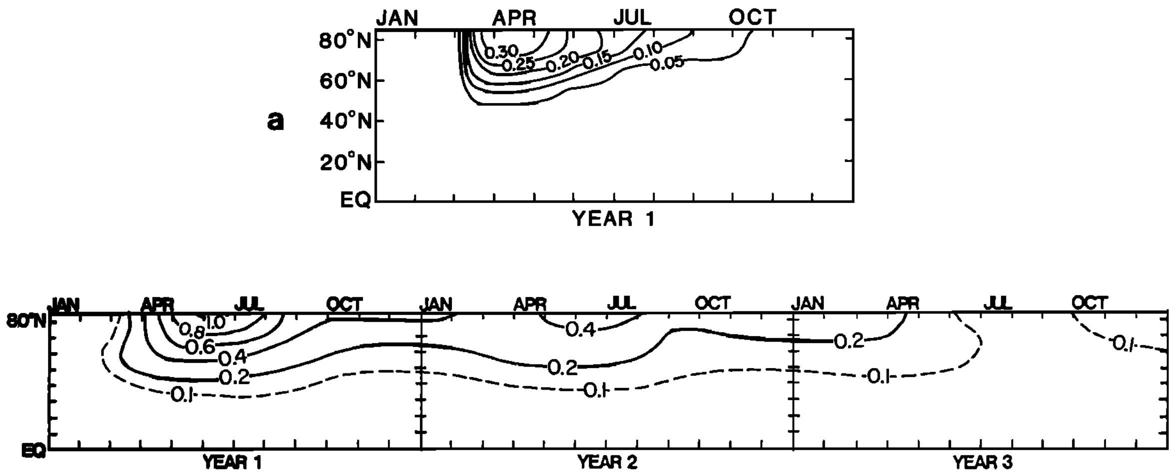

Fig. 6. The hemispherically distributed TTAPS scenario started in January. (*a*) Zonally averaged difference between the surface albedos (nuclear winter run with clean snow minus run with dirty snow, the "albedo difference"). Years 2 and 3 and southern hemisphere not shown because differences there are small, less than 0.05. (*b*) Zonally averaged difference between the surface air temperatures (in degrees Celsius) (nuclear winter run with dirty snow minus run with clean snow, the "cooling reduction"). Southern hemisphere not shown because differences there are small, less than 0.01°C.

but a small component is also due to changes in the snow and ice areas and to different temperatures (affecting the albedos via the meltwater mechanism) There is no large albedo difference in the second year, since most of the smoke has already been removed from the atmosphere, and its possible reappearance is not modeled here The difference in the surface air temperature between the clean and dirty snow nuclear winter model runs is given in Figure 6*b* which indicates that the dirty snow reduces the nuclear winter cooling at the pole by 1.0°C. The maximum "cooling reduction" occurs in June, when the incident solar radiation is greatest, not in January, when the dirty snow albedo difference is greatest. This illustrates the importance of the seasonally dependent solar radiation At the pole the maximum cooling reduction (1.0°C) reduces the clean snow nuclear winter cooling by 44% (compare Figure 5 to Figure 6*b*). At 60°N the maximum cooling reduction (0.5°C) is a 20% "relative cooling reduction" in the first year ("relative," that is, to the clean snow nuclear winter cooling). A cooling reduction continues into the second year, where there is no large albedo difference to support it. This extended cooling reduction is caused by the thermal inertia of the system which retains some of the initial dirty snow cooling reduction.

The NRC scenario is started in January and spread uniformly over the northern hemisphere. The albedo difference and the accompanying cooling reduction are given in Figures 7*a* and 7*b*. The NRC albedo differences are smaller and not as long-lived as the TTAPS albedo differences and, for this reason, the NRC cooling reductions are also smaller than the TTAPS cooling reductions. The maximum NRC cooling reduction at the pole, 0.8°C, causes a relative cooling reduction of 80%. The maximum cooling reduction at 60°N (0.35°C) causes a relative cooling reduction of 30%. Note that the cooling reductions in both the NRC and TTAPS scenarios are mainly constrained to the small area poleward of 60°N. The maximum relative cooling reductions at the

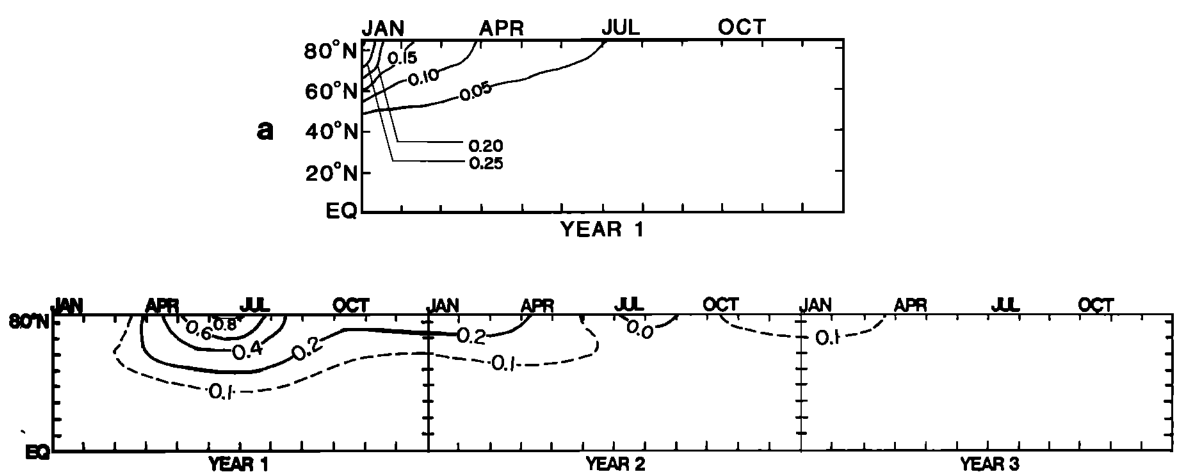

Fig. 7. As in Figure 6, but for the hemispherically distributed NRC scenario started in January.

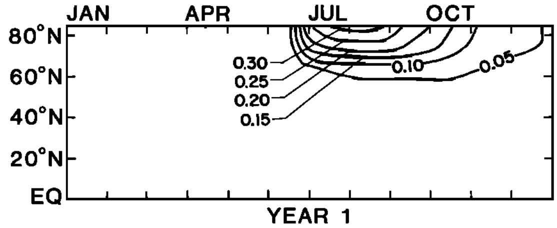

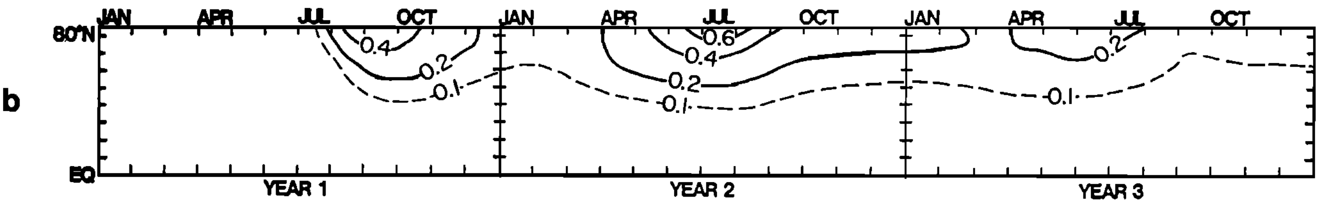

Fig. 8. As in Figure 6, but for the hemispherically distributed TTAPS scenario started in July.

pole are greater for the NRC scenario (80%) than for the TTAPS scenario (44%), mostly because there is much less nuclear winter cooling in the NRC scenario but also since the smoke cloud is more transparent to solar radiation, which allows more radiation to reach the surface to be absorbed The importance of the smoke cloud's absorption of solar radiation to the temperature effect of the dirty snow is discussed later

The TTAPS scenario causes the greater absolute cooling reductions so, for illustration, this forcing is used to investigate the effects of the dirty snow for different seasonal timings

5.5. *Seasonal Dependence*

The hemispherically distributed TTAPS scenario is started at different times of the year to examine the seasonal dependence of the dirty snow forcing

The albedo difference between the clean and dirty snow runs of the July forcing is given in Figure 8*a*. These albedo differences have a smaller spatial extent than in the hemispherically distributed January case (compare Figure 6*a* and Figure 8*a*) because of the smaller summertime snow and ice areas (not shown) Hence the maximum cooling reduction in the July case (0.7°C, see Figure 8*b*) is smaller than that in the January case (1.0°C). The maximum cooling reduction for the July case occurs in the second year, when the atmosphere is cleaner and the dirty snow does not cause a detectable albedo difference. This is obviously not a direct albedo effect, but a nonlinear model response due to the reduced thermal inertia and meltwater feedbacks

Another factor which influences the dirty snow effect is the climatological cloud cover in the polar region in the northern hemisphere summer (80–90%). Should the cloud coverage decrease markedly in a nuclear winter, the cooling reduction caused by the dirty snow albedos would be larger

When the hemispherically distributed TTAPS forcing is started in October (not shown), the dirty snow causes the smallest cooling reduction, even though its albedo differences are larger than in the July case. This is because the maximum albedo difference occurs when the solar insolation is a minimum in the northern hemisphere.

The maximum dirty snow effect occurs when the forcing is started in late March. For this seasonal timing the albedo differences are largest (due to the larger snow and ice areas) at the same time the solar insolation is increasing (Figure 9*a*). This yields the greatest cooling reductions at the pole of 2.2°C the first year, and 0 6°C in the second year (Figure 9*b*). In this case, the effects at the mid-latitudes are much greater than in the previous experiments. This is particularly evident in the cooling reduction over the more sensitive land areas (Figure 9*a*) The zonally averaged relative cooling reductions at the poles are 42% the first year and 38% the second year (compare Figure 9*b* to Figure 9*d*). At 60°N the maximum cooling reductions of 0.9°C the first year and 0.4°C the second year represent relative cooling reductions of 16% and 13%, respectively The cooling reductions here, as in the previous dirty snow cases, still have a shorter duration than the nuclear winter cooling (given in Figure 9*d*) When the precipitation rate of 30 kg m^{-2} $month^{-1}$ is used (not shown), the relative cooling reductions at the pole are 23% the first year and 20% in the second.

5.6. *Smoke Cloud Absorption*

Warren and Wiscombe [1985] stated that the surface albedos may not be very important until the atmosphere has lost most of its light-absorbing smoke. The objective of this section is to quantify the importance of the smoke cloud at reducing the temperature effects of the dirty snow.

The hemispherically distributed TTAPS scenario, started in March, was used for this test, since it produces the maximum dirty snow effect. In this experiment the climate model was run, as before, with the nuclear winter smoke cloud in place for the clean and dirty snow cases, and the surface albedos for each case were saved (The "surface albedos" saved include information about the actual albedos and the cryospheric areas produced.) The model was then run with a clean atmosphere while using the saved clean and dirty snow albedos Comparing the temperature differences (between the clean and dirty snow runs) of the clean and smoke cloud atmospheres, we can see how the same surface albedo difference can cause different temperature responses depending on whether a smoke cloud is present or not.

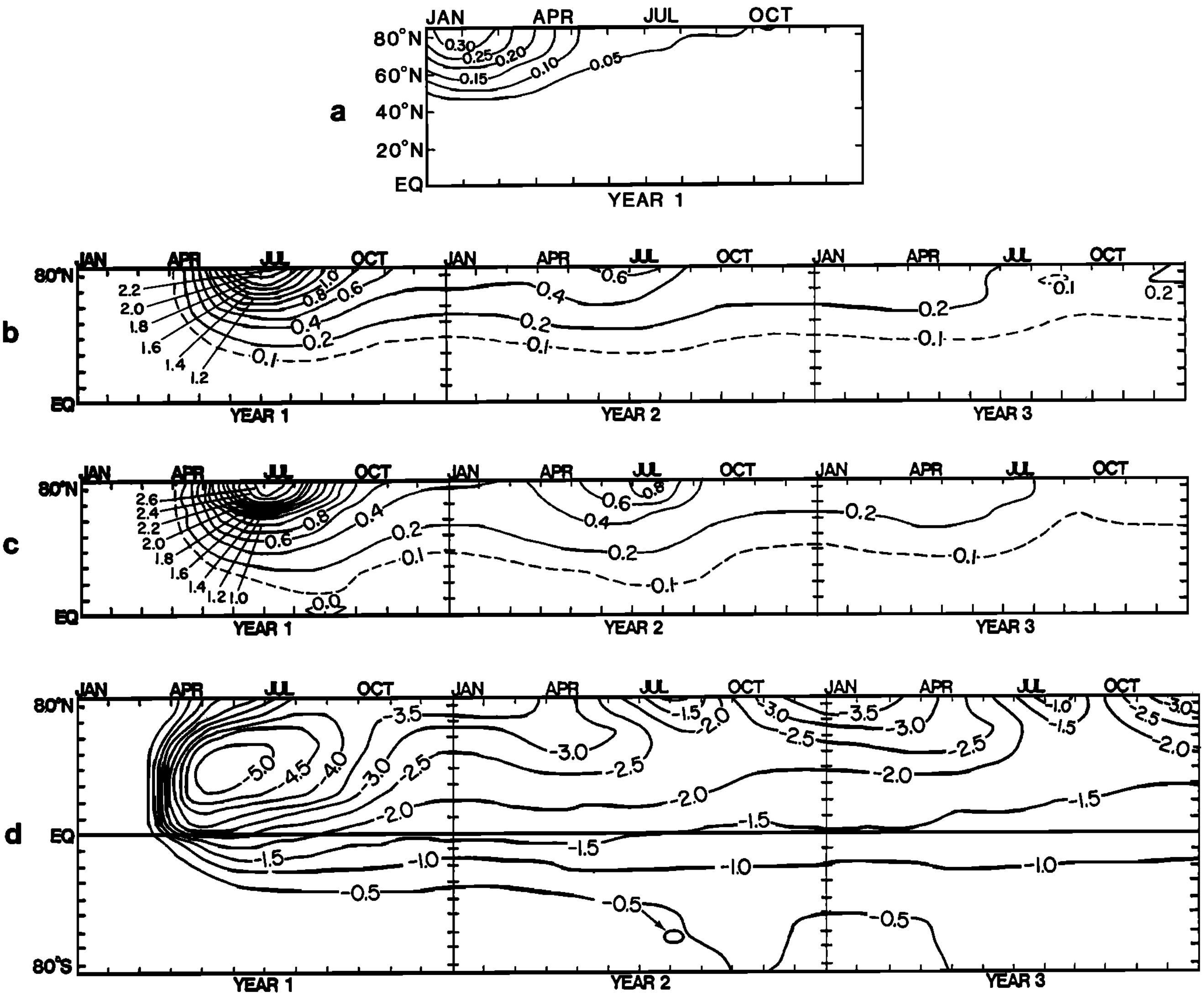

Fig. 9. (*a* and *b*) As in Figure 6, but for the hemispherically distributed TTAPS scenario started in March. (*c*) Cooling reduction zonally averaged only over the land areas. (*d*) Zonally averaged cooling (in degrees Celsius) when the dirty snow albedos are used (nuclear winter run with dirty snow minus unperturbed climate).

The temperature difference between runs with and without dirty snow in a clean atmosphere is given in Figure 10. As expected, the clean atmosphere temperature differences are much greater than the temperature differences in the smoke cloud atmosphere since the darker snow is able to absorb more solar energy incident at the surface. Comparing Figure 9*b* and Figure 10, the temperature difference caused by the dirty snow is increased by 82% when a smoke cloud is not present. This shows that the smoke cloud does, in fact, play a large role in reducing the short-term effect of the dirty snow albedos. It then also plays a large role in reducing the positive snow albedo surface temperature feedback in the first year.

5.7. *Soot Reappearance*

It is possible that the soot may reappear in later summers when the snow cover melts [*Warren and Wiscombe*, 1985; *Ledley and Thompson*, 1986]. This could be important, since small albedo differences in the later years could cause large temperature differences after the smoke cloud has dissipated and more solar radiation is made available at the surface for absorption. The albedo difference caused by the soot's reappearance in later years would probably be much smaller

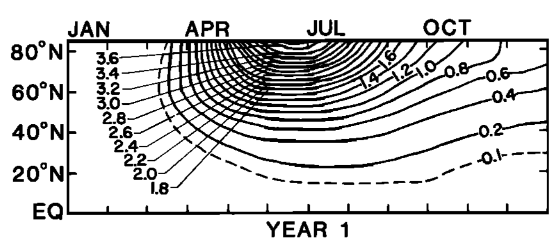

Fig. 10. Dirty snow effects in a clean atmosphere. Temperature difference (in degrees Celsius) between the "clean-atmosphere" runs which use the clean and dirty snow albedos saved from the nuclear winter runs (dirty snow run minus clean snow run). The albedo difference (between the clean and dirty snow albedos) is given in Figure 9*a*.

than its albedo difference in the first year because the soot could only reappear on permanent snow areas and multiyear sea ice areas which cover a relatively small area of the globe. Also, the soot could only reappear in the areas where the covering snow pack had melted enough to expose the soot. In the current climate the snow on the Arctic sea ice melts completely in the summer [*Warren and Wiscombe*, 1985]. This, however, is in the absence of the nuclear winter cooling and the cryospheric feedbacks which could both increase the snow and ice packs and hinder their subsequent melting. Eventually, the soot would probably be buried permanently by snow or ice, like the volcanic ash deposits and other impurities found in glacial ice cores [*Warren*, 1984].

The possible effects of the soot in later years are investigated using a simple reappearance parameterization. Of particular interest is how this reappearance (after the smoke cloud has dissipated) interacts with the long-term cooling controlled by the thermal inertia of the ocean and the cryospheric feedbacks. The maximum long-term dirty snow effect would be achieved when the smoke is quickly removed from the atmosphere (as in the January case of *Malone et al.* [1986]). In this case the nuclear winter cooling is minimized as is the long-term cooling controlled by the cryospheric feedbacks and the ocean's thermal inertia. This would also cause a greater concentration of soot in the snow pack, since the smoke is deposited in a shorter period of time. Since the smoke is quickly washed out of the atmosphere in the NRC scenario (62% removed the first month and 78% by the end of the second month), it was chosen to simulate this situation. This forcing was started in March and was hemispherically distributed to achieve the maximum dirty snow effect

To approximate the possible reappearance of the soot, the meltwater albedo was maintained at its lowest NRC value (0.23), while the dirty snow albedos changed as indicated in Figure 2 (the baseline precipitation rate was used) During melting this parameterization reduces the snow and ice albedos to the lower meltwater value at a faster rate than if the snow were clean. Similar albedo changes could be expected if an underlying layer of soot were uncovered and brought to the surface. This parameterization overestimates the possible dirty snow albedo change, since the cryospheric areas which re-form after melting completely (thus discharging their soot content) are still assumed to have this dirty meltwater albedo This parameterization also assumes that the soot is always uncovered during melting and can never be concealed by the snow or ice pack. Although being an extreme, this parameterization may be more realistic in the second year than not allowing the soot to reappear at all

The albedo differences between the clean and dirty snow nuclear winter model runs are given in Figure 11*a* With this meltwater parameterization, the albedo differences in the later years (0 20) are almost equal in amplitude to the albedo differences in the first year The maximum albedo differences appear in the summertime, when the solar insolation and melting is greatest The albedo differences in the third year are probably unrealistically large (particularly in the mid-latitudes), since the snow and ice which had melted and re-formed would not have this dirty meltwater albedo. Figure 11*b* shows that large and persistent cooling reductions occur after the first year. The cooling of the nuclear winter run with dirty snow is given in Figure 11*c*. Figure 11*c* indicates that the soot reappearing in a clean atmosphere can actually cause warming at the pole as great as 1°C. The maximum dirty snow cooling reductions in the second year, relative to the clean snow nuclear winter cooling, are 110% at the pole and 55% at 60°N. Although this extreme dirty snow parameterization can cause anomalous warming, anomalous cooling can also exist in the wintertime at the poles more than 2 years after the nuclear winter forcing has stopped as well as in other regions.

To understand how this cooling is able to persist, the sea ice area feedback is examined. When the NRC nuclear winter forcing is applied with clean snow albedos, the sea ice areas increase as illustrated in Figure 11*d*. Figure 11*d* shows that in response to the nuclear winter cooling, 7 5% more of the total sea area is covered by ice When the dirty snow albedos are used with this reappearance parameterization, these sea ice areas are decreased by the amount given in Figure 11*e*. From these results, the dirty snow is able to decrease the anomalous ice areas by 30 to 50%, depending on the latitude and year after the start of the forcing. This suggests that the dirty snow albedos could play an important role in reducing the ice area feedback by opening the sea areas more quickly. But even with the persistent reappearance of soot, the anomalous ice areas still exist after the direct nuclear winter forcing has dissipated. The ice area feedback continues because it only requires cold temperatures to operate, while the dirty snow requires exposure to sunlight, which is hindered by snow coverage, and the blocking of sunlight by both smoke and water clouds

6 DISCUSSION

A global energy balance climate model was forced with the nuclear winter scenarios of TTAPS, NRC, and Malone et al The magnitude of the nuclear winter cooling caused by these forcings varied a great deal depending on the scenario used and the seasonal timing. With the exception of the January Malone et al scenario, the results show that long-term cooling was possible after the direct forcing had ended due to the cryospheric feedbacks and the ocean's thermal inertia These results show qualitative agreement between the current improved version of the climate model and that used by *Robock* [1984*b*], which neglected the downward infrared flux from the smoke cloud. The amplitude of the sustained cooling, however, is less than that suggested by *Robock* [1984*b*] and, with the present radiation scheme, warming can even occur at the pole in the winter.

The ability of the dirty snow to reduce this cooling was then investigated The dirty snow causes large albedo changes in the high latitudes in the first year which reduce the nuclear winter cooling at the pole by 8 to 80%, depending on the scenario used and the seasonal timing The relative cooling reductions at 60°N were approximately half those at the pole. The greatest factor affecting the relative cooling reductions was the varying magnitude of the nuclear winter cooling itself. The cooling reductions were greatest when the forcing was started in March and January, since the albedo changes were best correlated with the incident solar radiation. *Ledley and Thompson* [1986] also found this same seasonal sensitivity of the forcing in their dirty snow study on sea ice coverage.

In an experiment designed to maximize the dirty snow effect, the soot was allowed to continually reappear. In this

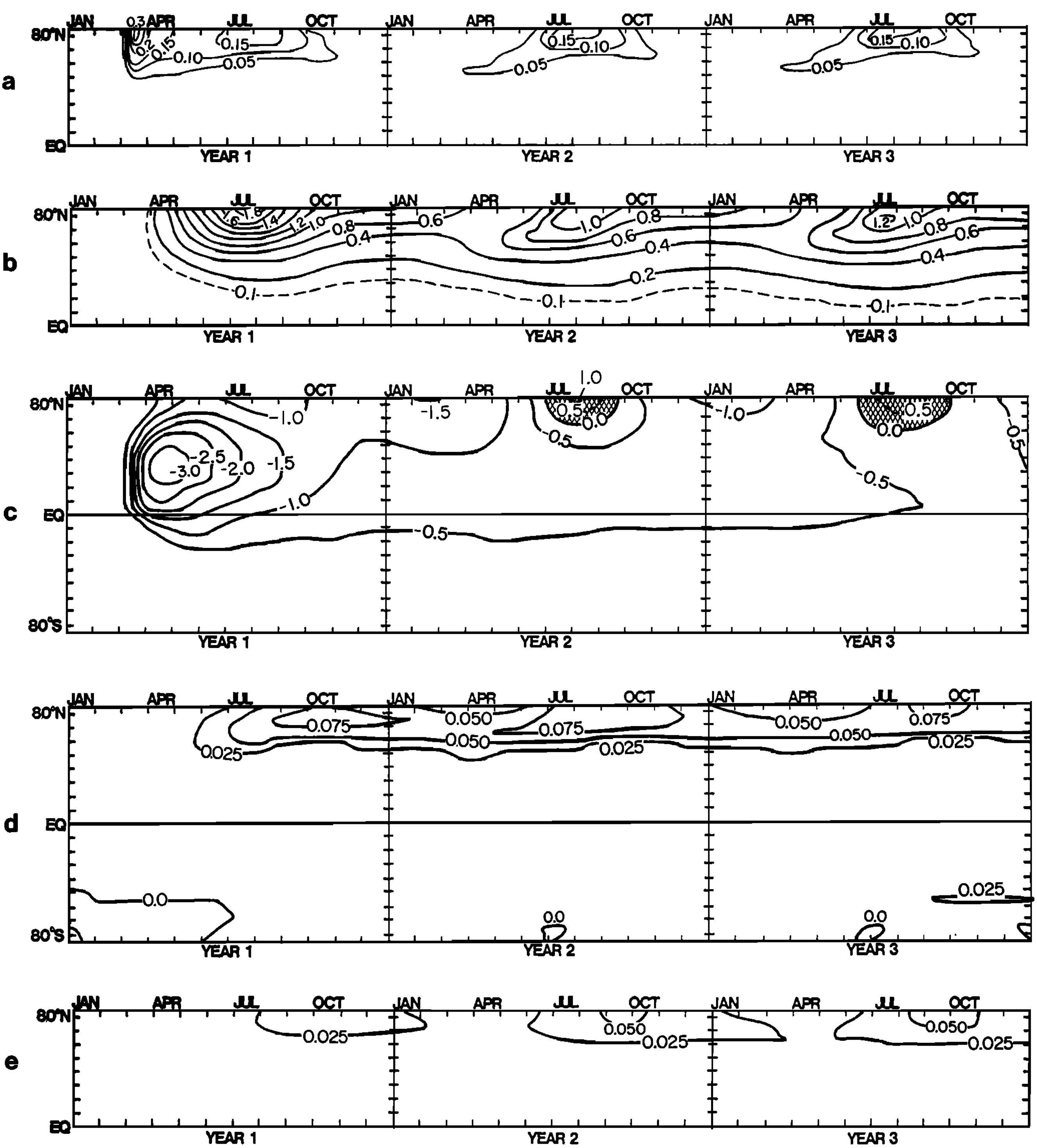

Fig. 11. (*a* and *b*) As in Figure 6, and (*c*) as in Figure 9*d*, but for the hemispherically distributed NRC scenario started in March, using the soot reappearance parameterization. (*d*) Sea ice area feedback. The increase in the fractional amount of the total sea area covered by ice in a nuclear winter (nuclear winter model run (with clean snow) minus climatology). (*e*) Sea ice area reduced by the dirty snow. The difference in sea ice coverage caused by the dirty snow (nuclear winter run with clean snow minus run with dirty snow).

extreme parameterization, the dirty snow was able to cause net warming on the order of 1°C at the poles. The anomalous sea ice areas (caused by the nuclear winter cooling) were reduced between 30 and 50%, depending on the latitude and time after the start of the forcing. This shows that the reappearance of dirty snow could lessen the importance of the ice area feedback. But with the continual reappearance of the soot, positive ice area anomalies still continued more than 2 years after the nuclear winter forcing had ended. This heightened the high latitude sensitivity, via the sea ice thermal inertia feedback, enabling the wintertime polar temperatures to be colder than climatology by 1°C, while the summertime temperatures were warmer than climatology by about the same amount.

The results of Ledley and Thompson showed that the dirty snow could cause open oceans at 82 5°N for periods of 1.4–3.5 months. Our model results, however, show that even with the soot reappearance parameterization, there is still 5% more sea area covered by ice at that latitude. This discrepancy can mostly be explained, since the model used by Ledley and Thompson could not consider the effects of the smoke cloud in decreasing the solar radiation incident at the surface, the accompanying surface cooling, and, especially, the cryospheric feedbacks, which were all shown in this study to be important. Also, the sea ice model used by Ledley and Thompson does not calculate the fraction of the sea area covered by ice at each latitude, and their model cannot thermodynamically support ice south of 67.5°N [*Ledley and Thompson*, 1986] This may make their ice cover more sensitive to the dirty snow forcing Other differences between these studies are that the dirty snow albedos used here are higher than those used by Ledley and Thompson This is because the smoke in this study was deposited over a longer period of time in a manner consistent with its atmospheric residence time, and our interpolation of albedo curves from the results of *Warren and Wiscombe* [1985] assumed that the dirty snow albedos changed less with soot content than the interpolations done by Ledley and Thompson

A wide range of effects was considered with the dirty snow forcings. The results shown here are dependent on the present model's sensitivity to the forcing and on many assumptions and parameterizations which do not explicitly treat all of the complicated processes involved in simulating nuclear winter or dirty snow forcings

In the experiments shown here, cases were chosen to maximize the dirty snow effect If a higher precipitation rate were used (resulting in a lower soot concentration and smaller albedo reduction) or if the total sootfall were restricted more to the mid-latitudes, the dirty snow effects would be even less. If the climate model were more sensitive, in line with GCMs, then the sea ice thermal inertia feedback would be even larger and might be even more dominant over the dirty snow effect.

In conclusion, the net result of these experiments is that the effect of dirty snow can be very large at the poles, particularly if the soot is able to significantly reappear in later summers. The effect at the lower latitudes (60°N), however, is much weaker. The long-term importance of the dirty snow is particularly dependent upon the initial magnitude of the nuclear winter cooling, which strongly influences the long-term cooling controlled by cryospheric feedbacks and by the thermal inertia of the ice-free areas The long-term dirty snow effect is relatively small on the global climate, unless it is able to significantly reappear in later summers

There are three primary factors which limit the importance of the dirty snow. One is that the albedo change is greatest when there is still a large amount of smoke in the atmosphere, thereby only allowing a small amount of the incident solar radiation to reach the surface. (The water cloud cover also reduces the amount of solar energy which can be absorbed at the surface by the lower albedo.) The second factor is that the cryospheric feedbacks are still able to produce larger ice areas which help maintain colder temperatures via the thermal inertia feedbacks. The last factor is that the soot can only have a significant albedo effect on the small areas covered by snow and ice. These areas are greatest, however, when the seasonal solar radiation is a minimum.

Acknowledgments. We thank Huug van den Dool and Mike MacCracken for useful comments on the manuscript. We also thank Steve Ghan, for providing unpublished GCM data; Rich Turco, for scenario information; and Steve Warren, for papers he provided on snow albedo studies. The NASA/GLA Amdahl 470/V6 computer and the Department of Meteorology Apollo network were used to do the computations and word processing of this work. This research was supported by NSF grant ATM-8213184 and NOAA grant NA84AA-H-00026.

REFERENCES

Chylek, P., V. Ramaswamy, and V. Srivastava, Albedo of soot-contaminated snow, *J. Geophys. Res.*, *88*, 10,837–10,843, 1983.

Covey, C., Protracted climatic effects of massive smoke injections into the atmosphere, *Nature*, *325*, 701-703, 1987.

Crutzen, P. J., and J. W. Birks, The atmosphere after a nuclear war: Twilight at noon, *Ambio*, *11*, 114–125, 1982.

Ghan, S. J., M. C. MacCracken, and J. J. Walton, The climate response to large summertime injections of smoke into the atmosphere: Changes in precipitation and the Hadley circulation, IAMAP/IAPSO Joint Assembly, Honolulu, Hawaii, Rep. *UCRL-92324*, Lawrence Livermore Nat. Lab., Livermore, Calif., Aug., 1985.

Lacis, A. A., and J. E. Hansen, A parameterization for the absorption of solar radiation in the Earth's atmosphere, *J. Atmos. Sci.*, *31*, 118–133, 1974.

Ledley, T. S., and S. L. Thompson, Potential effect of nuclear war smokefall on sea ice, *Clim. Change*, *8*, 155–171, 1986.

Malone, R. C., L. H. Auer, G. A. Glatzmaier, and M. C. Wood, Nuclear winter: Three-dimensional simulations including interactive transport, scavenging and solar heating of smoke, *J. Geophys. Res.*, *91*, 1039–1054, 1986.

Manabe, S., and R. J. Stouffer, Sensitivity of a global climate model to an increase of CO_2 concentration in the atmosphere, *J. Geophys. Res.*, *85*, 5529–5554, 1980.

National Research Council, Committee on the Atmospheric Effects of Nuclear Explosions, *The Effects on the Atmosphere of a Major Nuclear Exchange*, 193 pp., National Academy Press, Washington, D.C., 1985.

Pittock, A. B., T. P., Ackerman, P. J. Crutzen, M. C. MacCracken, C. S. Shapiro, and R. P. Turco, *Scientific Committee on Problems of the Environment 28, Environmental Consequences of Nuclear War*, Vol. I: *Physical and Atmospheric Effects*, 359 pp., John Wiley, New York, 1986.

Robock, A., The seasonal cycle of snow cover, sea ice and surface albedo, *Mon. Weather Rev.*, *108*, 267–285, 1980.

Robock, A., The Mount St. Helens volcanic eruption of 18 May 1980: Minimal climatic effect, *Science*, *212*, 1383–1384, 1981.

Robock, A., Ice and snow feedbacks and the latitudinal and seasonal distribution of climate sensitivity, *J. Atmos. Sci.*, *40*, 986–997, 1983.

Robock, A., Climate model simulations of the effects of the El Chichón eruption, *Geofis. Int.*, *23*, 403–414, 1984*a*.

Robock, A., Snow and ice feedbacks prolong effects of nuclear winter, *Nature*, *310*, 667–670, 1984*b*.

Robock, A., Detection of volcanic, CO_2 and ENSO signals in surface air temperature, *Adv. Space Res.*, *5* (6), 53–56, 1985.

Sagan, C., and J. B. Pollack, Anisotropic nonconservative scattering and the clouds of Venus, *J. Geophys. Res.*, *72*, 469–477, 1967.

Sellers, W. D., A new global climatic model, *J. Appl. Meteorol.*, *12*, 241–254, 1973.

Sellers, W. D., A reassessment of the effect of CO_2 variations on a simple global climatic model, *J. Appl. Meteorol.*, *13*, 831–833, 1974.

Stephens, S. L., J. G. Calvert, and J. W. Birks, Ozone as a sink for atmospheric carbon aerosols: Today and following nuclear war, *Aerosol Sci. Technol.*, in press, 1988.

Thompson, S. L., S. H. Schneider, F. Giorgi, C. Covey, and V. Ramaswamy, Atmospheric effects of nuclear war aerosols in GCM simulations, paper presented at the Defense Nuclear Agency Global Effects Program Technical Review at NASA Ames Research Center, Moffett Field, Calif. February 25, 1986.

Turco, R. P., O. B. Toon, T. Ackerman, J. B. Pollack, and C. Sagan, Nuclear winter: Global consequences of multiple nuclear explosions, *Science*, *222*, 1283–1292, 1983.

Warren, S. G., Optical properties of snow, *Rev. Geophys.*, *20*, 67–89, 1982.

Warren, S. G., Impurities in snow: Effects on albedo and snowmelt, *Ann. Glaciol.*, *5*, 177–179, 1984.

Warren, S. G., and W. J. Wiscombe, A model for the spectral albedo of snow, II, Snow containing atmospheric aerosols, *J. Atmos. Sci.*, *37*, 2734–2745, 1980.

Warren, S. G., and W. J. Wiscombe, Dirty snow after nuclear war, *Nature*, *313*, 467–470, 1985.

R. G. Ellingson and A. Robock, Department of Meteorology, University of Maryland, College Park, MD 20742.

A. M. Vogelmann, Atmospheric and Environmental Research, Incorporated, 840 Memorial Drive, Cambridge, MA 02139.

(Received June 12, 1987;
revised January 15, 1988;
accepted January 18, 1988.)